Measurement of Anthropogenic Gadolinium in the Scioto and Olentangy River System Using Inductively Coupled Plasma Mass Spectrometry (ICP-MS)

Undergraduate Research Thesis

Submitted in partial fulfillment of the requirements for graduation

with research distinction in Earth Sciences

in the undergraduate colleges of

The Ohio State University

By

Cole E. Bradley

The Ohio State University

2018

Approved by

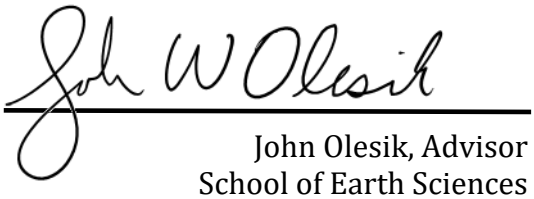

John Olesik, Advisor
School of Earth Sciences

TABLE OF CONTENTS

ABSTRACT

Gadolinium, a rare earth element (REE), is used throughout modern medical facilities as a paramagnetic component for Magnetic Resonance Imaging (MRI) contrast agents. Eventually after use, contrast agents travel through hospital or city wastewater treatment facilities and end up as waste in the City of Columbus's Scioto and Olentangy River systems. Our study, using inductively coupled plasma mass spectrometry, measured the dissolved rare earth element chemistry upstream, within the City of Columbus, and downstream of the City of Columbus's wastewater treatment facilities to detect any possible amounts of anthropogenic gadolinium throughout these waterways. Following the detection of any anthropogenic gadolinium, we sought to identify if the City of Columbus has any impact on the concentration of anthropogenic gadolinium and if so, at what relative concentrations. Through our study, were able to detect anthropogenic gadolinium directly downstream of the City's wastewater treatment facilities, indicating the City of Columbus does have an influence on existing concentrations of gadolinium. The estimated concentrations of anthropogenic gadolinium measured downstream of Columbus wastewater treatment plants ranged from 0.025 ppb to 0.040 ppb (part per billion, μg/L).

ACKNOWLEDGEMENTS

I could never imagine myself where I am today if it were not for the countless mentors I've had throughout my studies. Specifically, I would like to thank Dr. John Olesik for his guidance and breadth of knowledge when it came to creating an exciting and meaningful research opportunity. Dr. Olesik always knows how to take a project from its big picture and break it into several easily understandable pieces that make the whole process obtainable and less intimidating. I would also like to thank Anthony Lutton for his guidance in standard preparation, experiment planning, and over all friendship along the way. My days in the lab would not have been as cheery without you. Dr. Anne Carey's direction and guidance throughout my undergraduate experience always kept me on the right path, helping to ease any worries that I had for my approaching years and research thesis project. I am incredibly thankful for both my mother and father for instilling a deep sense of creativity and curiosity into my life from the earliest of days. Their never-ending support and encouragement has always directed me to work towards the things that I love and make me happy, whatever they would be. Keith Karr, my stepfather, also with his endless support in life always drove me to work hard in school, informing me "The only thing that no one can take away from you is your intelligence...". Throughout my two years at The Ohio State University I have met a great group of friends. From working on labs until 2am, to hiking through the endless deserts & mountains of Utah together, we created memories that I will never forget. I would like to thank the whole School of Earth Sciences for creating such a great opportunity and home for all of the students; the knowledge I have obtained here is priceless and will forever guide the way I think. Lastly, I am unbelievably lucky to have gained financial support throughout my undergraduate experience from the Lieberman Scholarship fund, the Arts and Sciences Scholarship, SES Field Experience Travel Funding, and the Sharp Memorial Scholarship, without this help, I would still be working in a restaurant dreaming about college.

List of Figures

List of Tables

INTRODUCTION

Gadolinium is commonly used as a paramagnetic component for enhanced contrast in Magnetic Resonance Imaging (MRI). MRI contrast agents improve image resolution and are composed of a strong paramagnetic metal atom bound to an organic molecule through chelation for stability as it passes through the body (Bellin & van der Molen, 2008). There are several gadolinium-based contrast agents available (Bellin & van der Molen, 2008). Contrast agents are estimated to be used in 40 to 50% of all MRIs conducted (Bellin & van der Molen, 2008). A patient weighing 141 lbs, will on average be intravenously injected with 1 g of a gadolinium-based contrast agent for a single MRI procedure (Bellin & van der Molen, 2008). Following an MRI procedure, patients will naturally evacuate most of the gadolinium-based contrast agent through urine as a dissolved solid within 24 hours (Bellin & van der Molen, 2008). In Columbus, this waste then flows through either the hospital's wastewater treatment or the city's wastewater transport systems. The city's wastewater is transported to either the Southerly or the Jackson Pike wastewater treatment facilities along the Scioto River. Once the wastewater has been processed, it is then released back into the Scioto River.

Chemically, gadolinium is grouped into a category of elements named the rare earth elements (REE). REEs have been shown to exist in relatively similar concentration patterns to one another throughout most of the Earth's upper crust due to their igneous sourcing and the assumption that they are relatively immobile through natural weathering and transport processes (Humphris, 1984). These concentration patterns, marked by characteristic shale and chondrite standards (Figure 1, Table A1), allow us to estimate the expected natural relative concentrations of the REEs (Taylor & McLennan, 1985).

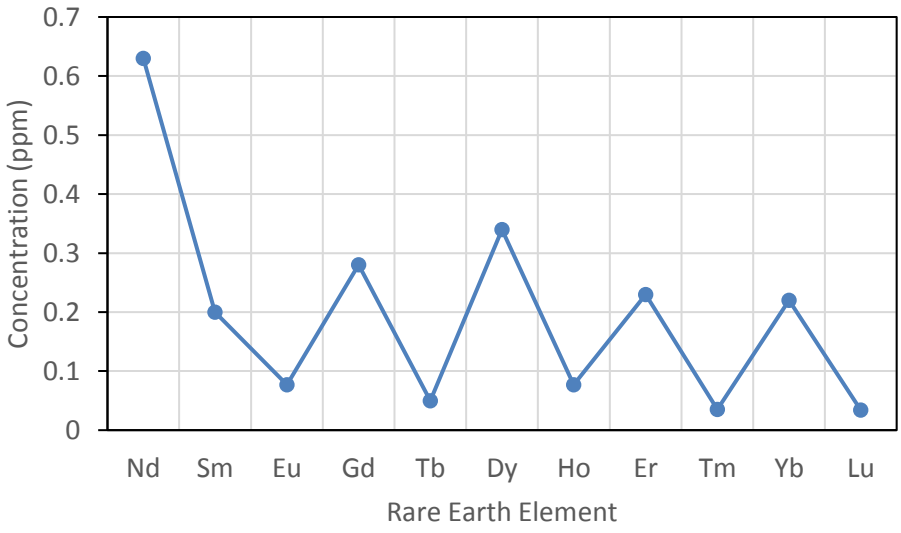

Figure 1. Rare earth element concentrations in a Chondrite standard (Longerich & Fryer, 1987).

The concentrations of REEs in water samples can be compared through a ratio to the expected natural relative concentrations in a chondrite or shale standard in order to identify any sharp deviations from the standard that may indicate if there is anthropogenic source of a particular REE. Previously published studies, using similar methods, have detected anthropogenic gadolinium within fresh water systems and also treated drinking water. A study conducted across the city of Berlin, Germany, where some drinking water sources are obtained through river-bank filtration, detect up to 180 ppt (part per trillion, ng/L) of anthropogenic gadolinium in certain locations (Kulaksiz & Bau, 2011). From a region within the United States, a study conducted in San Francisco California, detected up to 17.6 ppt of anthropogenic gadolinium throughout the San Francisco bay (Hatje et. al., 2016). Other studies from around the world include (Bau & Dulski, 2006) where anthropogenic gadolinium was detected amongst the great lakes and also Pennsylvanian rivers, and (Klaver et. al., 2014) where anthropogenic gadolinium was measured in the Rhine-Meuse River system in the Netherlands.

Our study measured the REEs throughout the Scioto and Olentangy River system of Ohio using inductively coupled plasma mass spectrometry (ICP-MS) to determine if the city's wastewater contributes anthropogenic gadolinium to the river water. Eleven separate locations throughout the Scioto and Olentangy Rivers were sampled (Figure 2). By sampling upstream of Columbus, within the City of Columbus, and downstream of the city's wastewater treatment plants we sought to determine where, if any, anthropogenic source of gadolinium occurred.

Geologic Setting

The Scioto and Olentangy River system exists within central Ohio's Scioto drainage basin (Figure 2). The Scioto drainage basin is underlain by multiple types of sedimentary bedrock units. In the northern and central regions, carbonates and shale dominate the underlying units, whereas in the southern regions, the bedrock geology is dominated by a mixture of shale, sandstone, and more carbonate. Amongst our entire sampling area of the Scioto and Olentangy River system, glacial deposits are found overlying nearly all of the bedrock units (Raab, 2005).

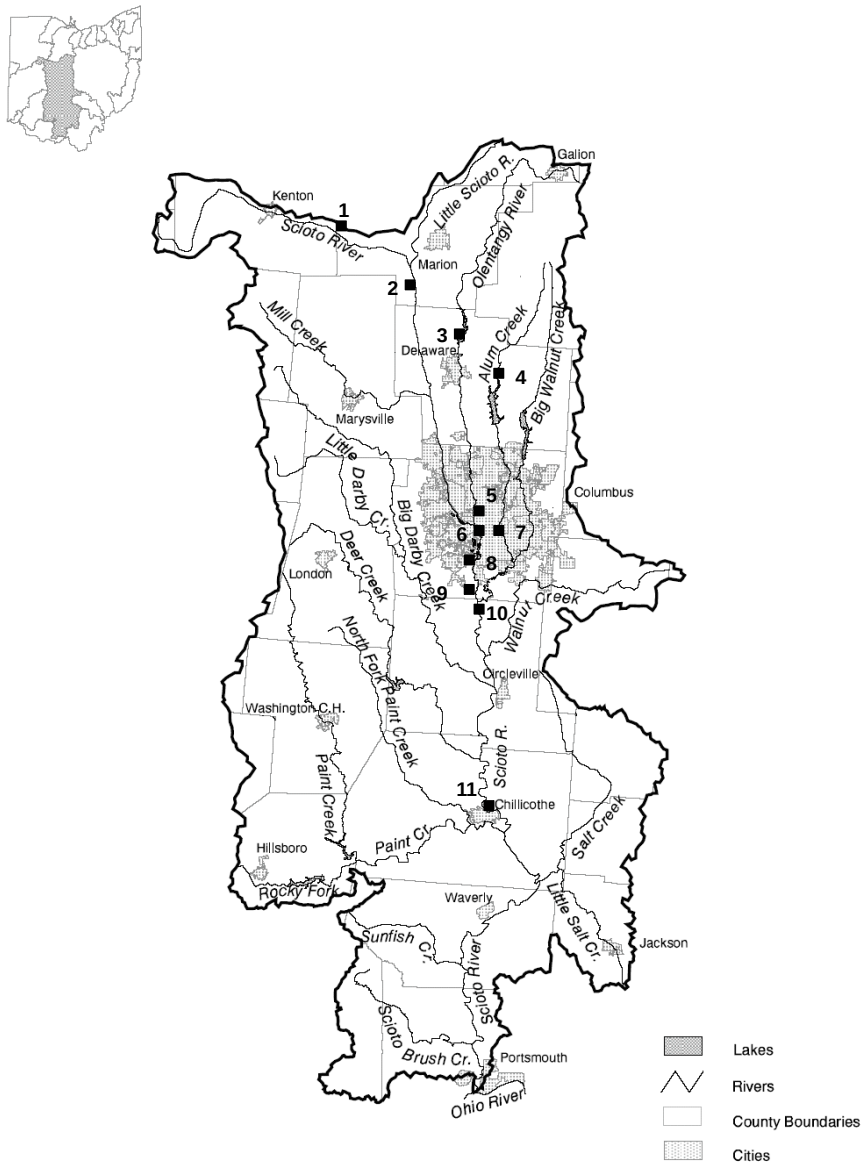

Figure 2. Map of sampling locations within the Scioto River Drainage Basin: (1) La Rue (LR), (2) Prospect (P), (3) Delaware Dam (DD), (4) Kilbourne (K), (5) Drake Union – The Ohio State University (D), (6) Battelle Riverfront Park (RF), (7) Bexley (B), (8) Jackson Pike WWTP (JP), (9) Southerly WWTP (S), (10) Commercial Point (CP), (11) Chillicothe (C). (Adapted from (Raab, 2005))

EXPERIMENTAL

Pre-sampling Preparations: On the morning of December 2nd 2017, twenty-seven one-liter, low-density polyethylene (LDPE) bottles were triple rinsed with deionized water. LDPE bottles were chosen as containers because of their low innate trace metal concentrations and their stability at temperatures less than 80°C (Gaines, N.D.). The bottles were then completely filled with deionized water. Each bottle was immediately stored in a two-liter sealable plastic bag which was then placed into a second two-liter sealable plastic bag. Five of these bottles served as field blanks throughout the sampling, sample preparation and analysis processes, allowing insight to any contamination occurrences that may have occurred throughout the study. The sealed sampling bottles were stored in plastic containers until sample collection later that morning.

Sampling: On December 2nd 2017, following the pre-sampling preparation, two one-liter water samples were collected from each of eleven separate locations of the Scioto and Olentangy River systems. Weather conditions throughout the week had been cloudy with some rain, while on that day they were mostly clear with some cloud coverage and no rain. The sampling areas were selected in close comparison to a past study conducted by Savelas Rabb (Raab, 2005) looking into the effects of urbanization on the Scioto River system. Figure 2 shows the adapted sampling locations. Aaron Hutchinson and I collected the water samples using the Clean Hands/Dirty Hands procedure (Fitzgerald & Davidson, 1999). Samples were collected from the main current of the river, roughly two to three meters out from the riverbank and about a half meter below the water surface. Field blanks were assigned to nearly every other sampling location. The field blank was opened using the Clean Hands/Dirty Hands procedure and was set on the riverbank while the water sample was collected. After collection, the field blank bottle was closed and sealed again by using the same procedure. Back at the vehicle, the outer sealed plastic bag was then labeled according to the sampling location and stored in the plastic containers. Upon returning to the lab, the samples were then stored overnight in their plastic containers. Three days after collection, each bottle was taken out of its sealed plastic bag, labeled, and refrigerated for future analysis.

Pre-Analysis Sample Preparation: On December 18th 2017, sample water was poured from each one-liter bottle to approximate a one-liter volume. The samples had been over filled during collection. 100 mL of each field blank was poured into a new triple-rinsed 125 mL LDPE bottle. Samples were then stored and refrigerated until January 2018.

On January 19th 2018, each of the water samples were poured into new, triple-rinsed 125 mL LDPE bottles, approximating 100 mL. Separate aliquots of each sample were poured and the pH of each sample was measured and recorded to detect any differences amongst the rivers electrochemistry (Table A2). All samples had very similar pH values, suggesting no significant difference throughout the river system.

On January 24th 2018, each sample was filtered through 0.2 μm pore size, 25 mm diameter hydrophobic filter attached to a 10 mL polypropylene & polyethylene syringe. First, in order to strip the hydrophobic coating on the filter, 10 mL of trace metal grade Methanol was flushed through the filter using the syringe. Next, to clean out both the syringe and filter, three 10 mL volumes of 2% volume/volume (v/v) trace metal grade HNO_3, followed by 10 mL of deionized water were pressed through the filter. After cleaning and rinsing the filter, 30 mL of sample was filtered into a triple rinsed 50 mL polypropylene centrifuge tube. This process was repeated for all samples, including the field blanks.

Isotopes and Calibration: On March 15th 2018, concentrations of the REEs in the collected water samples were measured using a Thermo Finnigan Element 2 inductively coupled plasma sector field mass spectrometer (ICP-SFMS). An Elemental Scientific PFA-100 nebulizer with an argon gas flow rate of 0.930 L/min and an Elemental Scientific PFA spray chamber with a sapphire injector were used. Instrument parameters consisted of a 1250 W RF power, plasma argon gas flow rate of 16 L/min, and an auxiliary argon gas flow rate of 1.0 L/min. The sample uptake rate was 100 μL/min and each isotope was measured over 1.3 seconds with 5 replicates per isotope.

A calibration blank solution (2% v/v trace metal grade HNO_3 in deionized water) was measured and its signal intensity was subtracted from the signals of the measured standards and water samples. Two lab-made standards, diluted with deionized water to concentrations of 0.100 ppb and 1.00 ppb from a 1.00 μg/mL (1 part per million) multi-element standard (PlasmaCAL–SCP Science) containing all of the REEs, were also measured. The sensitivity (signal/concentration) from the 0.10 ppb standard was 193 kcounts/s/ppb while the sensitivity from the 1.00 ppb standard was 133 kcounts/s/ppb. ICP-MS sensitivity should be independent of concentration particularly over a concentration range of one order of magnitude. Therefore, it is likely that the 0.100 ppb standard was contaminated; the signal produced from the 0.100 ppb standard is consistent with a concentration of 0.145 ppb. Therefore, the relationship between signal intensity (counts/s) and concentration was calibrated from the calibration blank and a 1.00 ng/mL (ppb) standard solution.

The isotopes with the highest natural abundances and likely the least significant amount of spectral overlap (Longerich et. al., 1987) were chosen to be measured (Table 1). Each of the elements were measured using a resolving power ($m/\Delta m$) of 300. Concentration measurements are shown in Table A3.

Table 1. Elemental isotopes measured.

^{141}Pr	^{143}Nd	^{145}Nd	^{147}Sm	^{149}Sm	^{151}Eu	^{153}Eu
^{156}Gd	^{157}Gd	^{158}Gd	^{160}Gd	^{159}Tb	^{163}Dy	^{164}Dy
^{165}Ho	^{167}Er	^{168}Er	^{169}Tm	^{173}Yb	^{174}Yb	^{175}Lu

Field Blanks & REE contamination in samples: ICP-SFMS signals from Field Blanks were 11x to 195x larger than the signals measured from the calibration blank (Table A4), which is also shown through the ratios of field blank signals to the calibration blank signals (Table A5). This suggests that the Field Blanks were contaminated either at some stage in the field or during the filtering process in the laboratory. If the contamination occurred in the field, the natural pattern of the relative REE concentrations would be expected amongst our field blanks. However, as shown in Figure 3 (and Table A6), the measured concentrations of the different REEs in the Field Blanks were very similar, rather than varying as expected in nature. The concentrations of Pr, Nd, Sm, Eu, Gd, Tb, Dy, Ho, Er and Tm are all between 0.016 and 0.018 ppb. This suggests that the contamination originated in the laboratory, particularly because the calibration standards contained equal concentrations of most of the REEs.

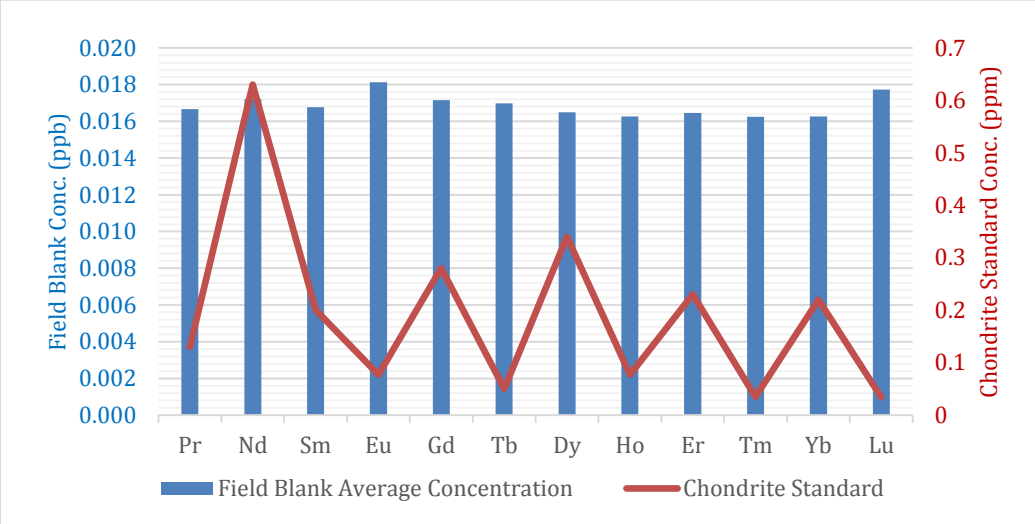

Figure 3. Average field blank concentrations compared to the chondrite standard concentrations.

Following the contamination discovery, new aliquots of the non-filtered field blanks were poured and analyzed on a later date and those showed no sign of contamination (Table A7). This analysis suggests that throughout the collection and storage process there was no contamination of the original samples and field blanks, only through sample preparation did they accumulate their contamination.

With this information, it is likely that the level of contamination in the processed samples is similar to that in the Field Blanks. Therefore, it may be reasonable to subtract the average concentrations of each REE in the Field Blanks from the average concentrations of each REE in the samples to account for the contamination and in particular, assess the pattern of REE concentrations. The possible range of gadolinium concentrations with and without Field Blank subtraction at each sampling location were determined and discussed in the Results and Discussion section.

Selection of REEs: Naturally occurring Tb, Ho, Tm and Yb are expected to have lower concentrations in the water samples than the other REEs, based on the relative concentrations of the REEs in the Chondrite standard (Figure 1, Table A1). In many of the river water samples, the concentrations of Tb, Ho, Tm and Yb are very similar to the average concentrations of these elements measured in the contaminated Field Blanks. Therefore, these elements were not included in subsequent assessment of the river water samples. Further, europium is known to suffer from a spectral overlap with barium oxide (BaO^+) (Jarvis et. al., 1989) and the concentration of Eu relative to other REEs can vary significantly in natural water due to oxidation state dependent fractionation (Bau, 1991). Therefore, we did not include Eu in further assessment. Last, a majority of the REE concentrations in samples from three locations (LaRue, Kilbourne and Bexley) were also very similar to the concentrations of most of the REEs in the contaminated Field Blanks. These three sample locations were not included in further assessment. Nd, Gd, Dy, Er and Yb are expected to have higher natural concentrations in the river samples than Tb, Ho, Tm and Yb, based on the concentrations in each of the Chondrite and Shale standards (Figure 1, Table A1). Consistently, the concentrations of these REEs were greater than their concentrations in the contaminated Field Blanks (Table A3). The final field blank subtracted concentration data selected for further analysis is shown in table A8.

Estimated Background Equivalent Concentrations (BECs): If all of the signal produced by the calibration blank is due to the presence of REEs as contaminants, this also need to be taken into account. By dividing these calibration blank signals by the sensitivity determined from the 1 ppb standard signal minus the calibration blank signal for each measured isotope, the background equivalent concentrations (BECs) were calculated. BECs quantify the concentrations of the background signal found within each sample at each isotope due to the measured calibration blank intensities. Our final BECs were multiplied by one thousand to produce ppt concentrations, shown in Appendix Table A9. Our calculated BECs are on average three orders of magnitude less than any measured concentrations, showing that there was very little interference due to our calibration blank.

Solid REE Standards: Three major solid standards represent Earth's upper crust REE concentrations, the Post-Archean average Austrailian shale (PAAS), the North American Shale Composite (NASC), and the European Shale Composite (ES). A solid Chondrite standard represents the primitive earth REE concentrations. All of the standard concentrations are shown in Table A1. By normalizing all of the shale standards to a Chondrite standard the overall relationship amongst the expected natural REE concentration patterns can be determined (Taylor & McClennan, 1985; Longerich & Fryer, 1987).

All of the Chondrite normalized standards show a very similar REE concentration pattern that varies smoothly as a function of mass, shown below in Figure 4. Overall, because this pattern remains consistent across all of the standards, the Chondrite normalized natural concentrations of REEs within the water samples are expected to be similar. If the Chrondrite normalized gadolinium ratio is higher than expected from

the pattern of REEs shown in Figure 4, then anthropogenic gadolinium is likely present.

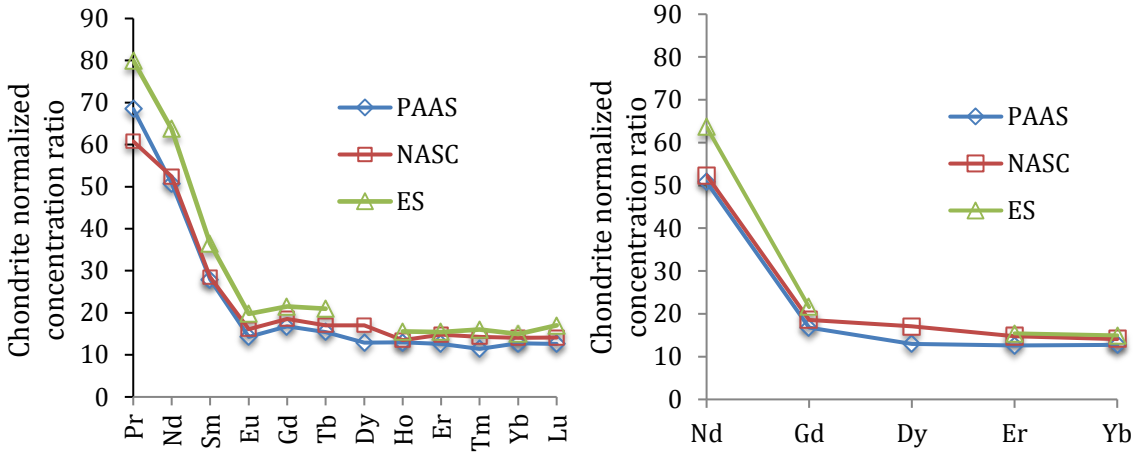

Figure 4. (A) Chondrite normalized REE concentration ratios in shale standards. **(B)** Chondrite normalized REE concentration ratios in shale standards for selected REE elements (most reliably measured in the collected river water samples).

Results and Discussion

Of the remaining eight sample locations, four were measured upstream or within the City of Columbus (Prospect, Delaware Dam, Drake Union, and Battelle River Front Park (Figure 5)) and four were measured downstream of Columbus (Jackson Pike WWTP, Southerly WWTP, Commercial Point, and Chillicothe (Figure 6)). The Scioto river system has a north to south flow direction, so, our chondrite normalized REE patterns are shown in order from the northernmost sample to the southernmost sample, and our total concentration figure reads from left (northernmost) to right (southernmost), following the flow direction of the river system. Separately, the REE chondrite normalized ratio patterns, the total measured gadolinium concentrations and the calculated anthropogenic gadolinium concentrations were all used for analysis.

REE concentration patterns upstream and within the City of Columbus: The chondrite normalized REE ratios measured upstream or within Columbus (Figure 5) mostly show a very smooth relationship, similar to that of the chondrite normalized shale standards shown in Figure 4B, representing the expected natural pattern. An exception to this is at the Drake Union location, which does show a slightly greater gadolinium ratio. This relationship suggests that there is no convincing evidence of anthropogenic gadolinium, perhaps with the exception of a small amount near Drake Union.

REE concentration patterns downstream of Columbus: The first water sample collected downstream of Columbus, which is just downstream of the Jackson Pike Wastewater Treatment Plant (Figure 6), shows a distinctly higher gadolinium ratio than other REEs. This heightened gadolinium ratio suggests the presence of an outside, anthropogenic source of gadolinium somewhere downstream of Battelle River Front Park but before the sampling location downstream of the Jackson Pike wastewater treatment plant.

Each of the samples collected further downstream also show this heightened chondrite normalized gadolinium concentration ratio. As we reach Chillicothe, the gadolinium ratio becomes lower than the other three downstream locations. This decrease in our gadolinium ratio could suggest some effect of dilution or that gadolinium is falling out of solution. Big Darby Creek, Walnut Creek, and Deer Creek are three major tributaries that merge into the Scioto River between our Southerly WWTP location and our furthest downstream location at Chillicothe (Figure 2), possibly contributing to the dilution and decrease in gadolinium ratio.

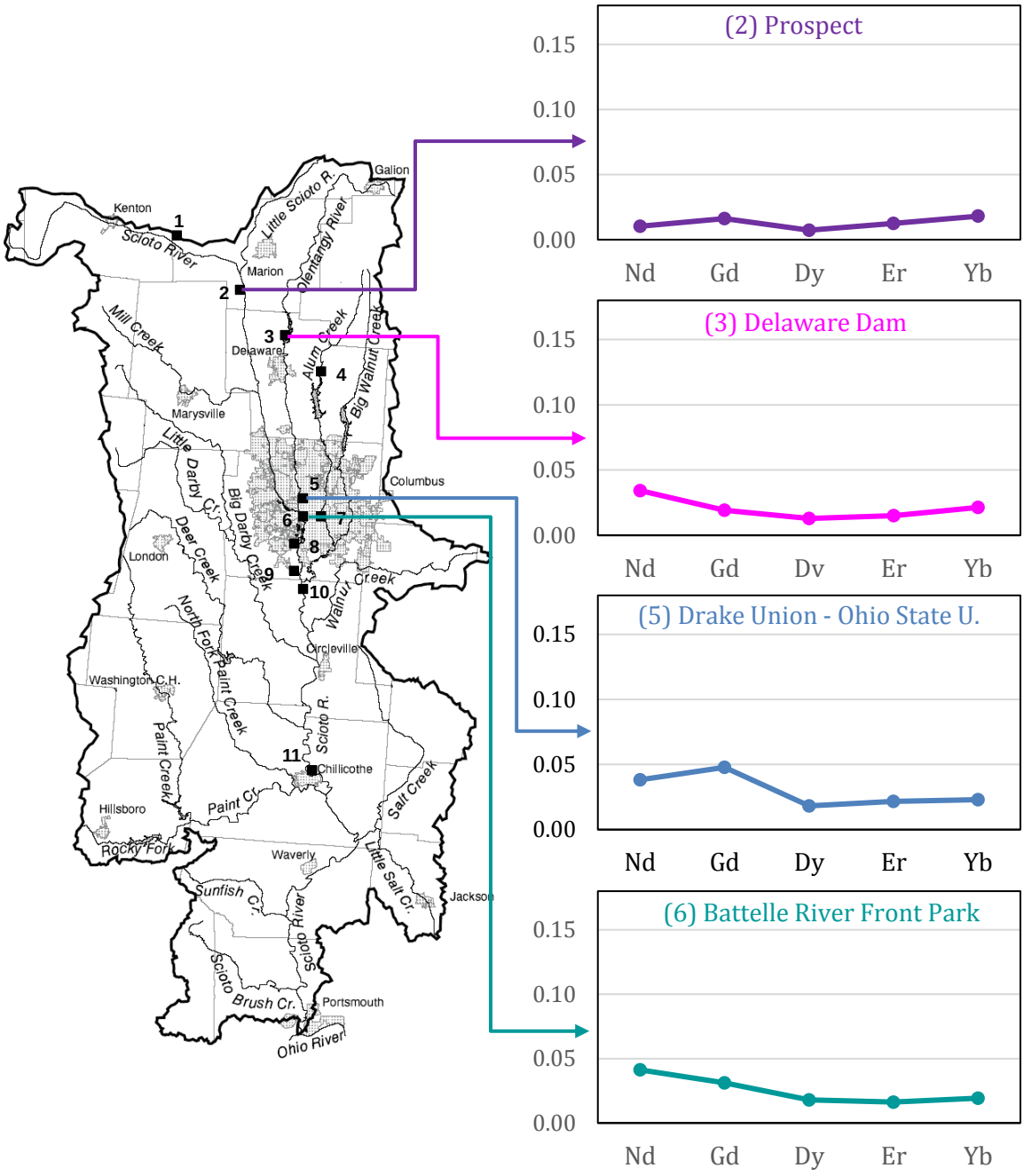

Figure 5. Chondrite normalized REE concentration ratios measured at locations upstream of Columbus (Prospect (2) and Delaware Dam (3)) and in Columbus (Drake Union – Ohio State University (5), Battelle River Front Park (6)).

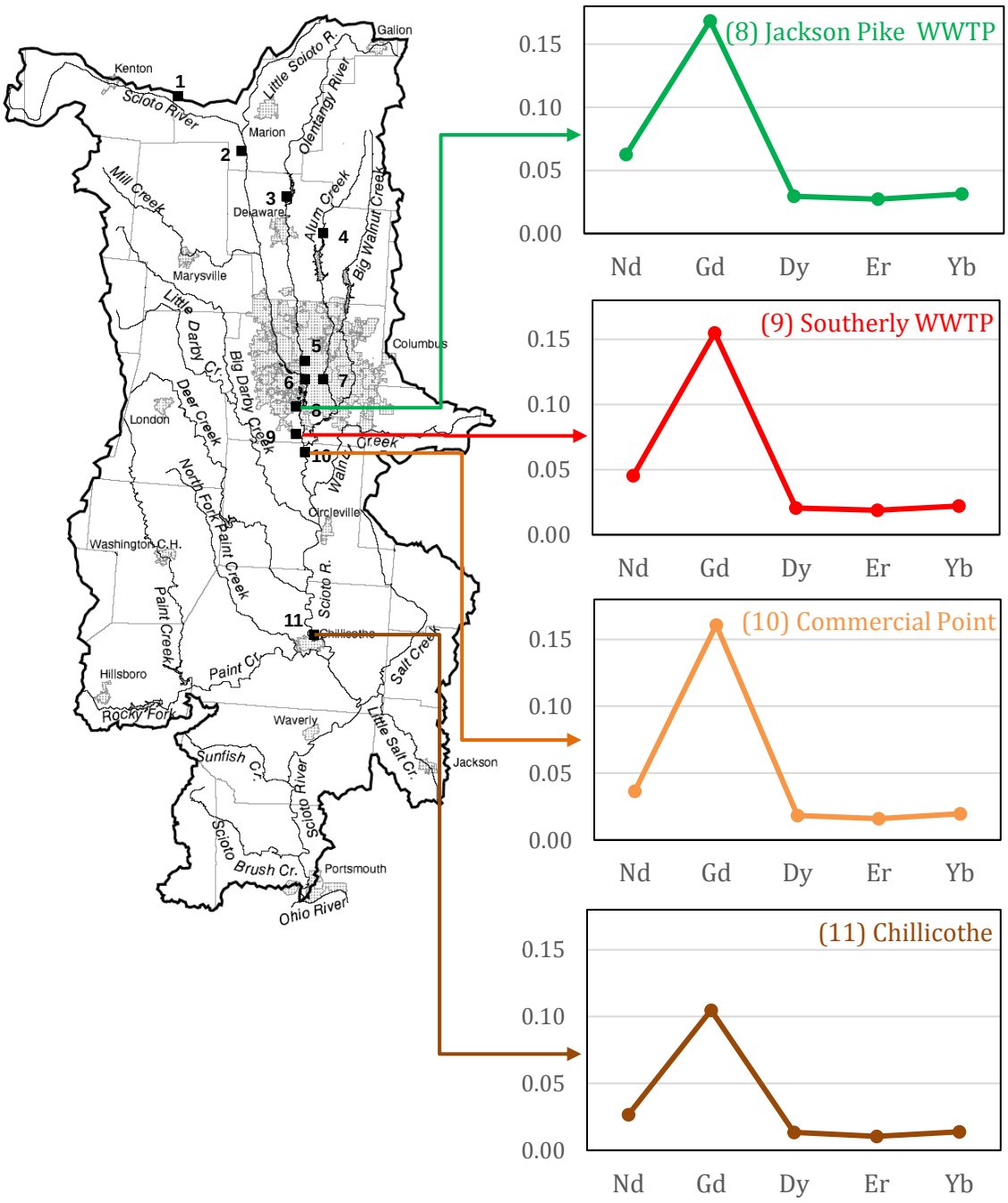

Figure 6. Chondrite normalized REE concentration ratios at locations downstream of Columbus (Jackson Pike WWTP (8), Southerly WWTP (9), Commercial Point (10), Chillicothe (11)).

Gadolinium Concentrations: The measured total (natural and anthropogenic) concentrations of gadolinium, with and without the subtraction of the average gadolinium concentration in the contaminated Field Blanks are shown in Figure 7 (Tables A3 and A8). The gadolinium concentrations are measured to be lower upstream of Columbus (Prospect and Delaware Dam) than within Columbus (Drake Union and Battelle River Front). Furthermore, there is a large jump in concentration from within the city at Battelle River Front Park to just downstream of Columbus' Jackson Pike Wastewater Treatment Plant. The field blank subtracted gadolinium concentrations increased from 0.009 ppb to 0.047 ppb and the gadolinium concentrations without field blank subtraction increased 0.026 ppb to 0.064 ppb.

These measurements indicate that there is an increase in gadolinium concentration from upstream of the city to within the city, and an even greater gadolinium concentration increase from within to city to downstream of the city's first wastewater treatment plant at Jackson Pike. This suggests that Columbus does influence the total gadolinium concentrations. The maximum concentrations are measured to be 0.047 ppb and 0.065 ppb, with and without Field Blank subtraction, respectively.

Downstream from the Jackson Pike WWTP there is a relatively consistent concentration until the Chillicothe location. There is a slight decrease in concentration at the Southerly sample location which may be due instrument detection limits. Overall, the average relative standard deviation of our measurements throughout all sample replicates is at 3%, showing a low amount of measurement variance.

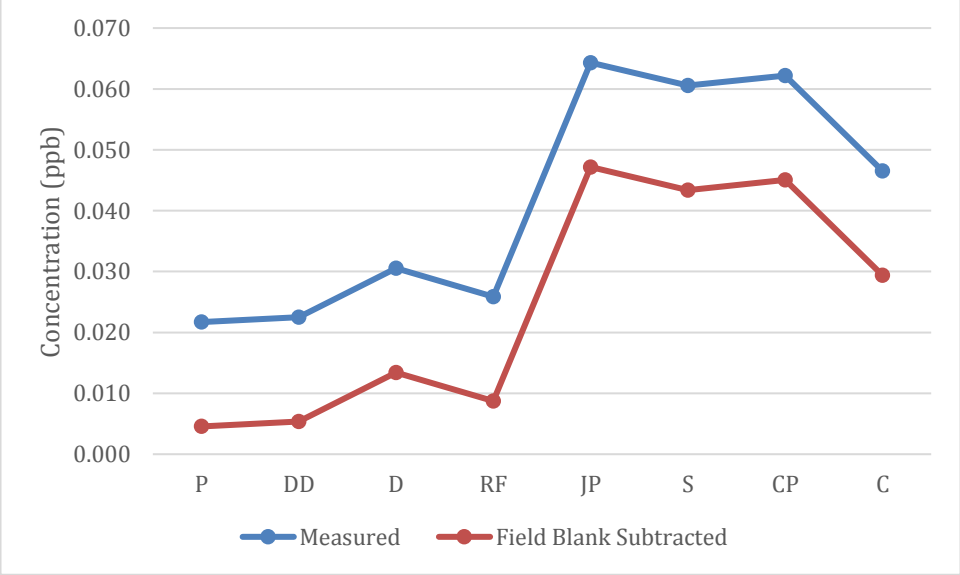

Figure 7. Measured and field blank subtracted gadolinium concentrations following the downstream direction of the Scioto and Olentangy River System. Sampling locations: Prospect (P), Delaware Dam (DD), Drake Union (D), Battelle River Front Park (RF), Jackson Pike (JP), Southerly (S), Commercial Point (CP) and Chillocothe (C).

Anthropogenic Gadolinium: The natural gadolinium concentrations at each sampling location can be estimated from the expected natural ratio of the gadolinium concentration to the concentration of another REE (assuming no anthropogenic source of the other REEs) and the measured concentration of that other REE. To make this estimation, the gadolinium concentration from natural sources, derived from the ratio of the gadolinium concentration to the concentration of a neighboring REE in the chondrite standard can be multiplying by the measured concentration of the same neighboring REE. The natural gadolinium concentration was estimated from the measured concentrations of Nd, Dy, Er, and Yb. The average estimated natural gadolinium concentration was then calculated for each location.

The average estimated natural gadolinium concentration at each location was subtracted from the total measured (natural and anthropogenic) gadolinium concentration to estimate the non-natural (anthropogenic) gadolinium concentration.

Table A10 and figure 8 show the estimated average anthropogenic gadolinium concentrations, both field blank subtracted values and non-subtracted values, from all of the downstream locations. Throughout the downstream locations, the anthropogenic gadolinium concentrations ranged from 0.025 ppb at Chillicothe to 0.039 ppb at Commercial Point from the field blank subtracted measurements, and from 0.028 ppb at Chillicothe to 0.040 ppb at Commercial Point without the field blank subtraction.

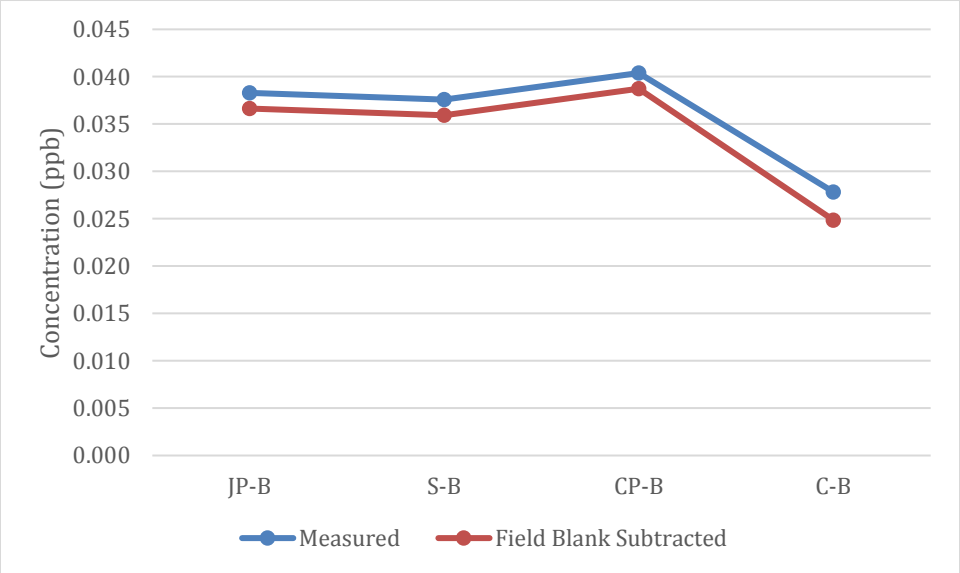

Figure 8. The measured and field blank subtracted estimated anthropogenic gadolinium concentrations downstream of Columbus.

CONCLUSIONS

The measured chrondrite normalized REE concentration ratios indicate the presence of anthropogenic gadolinium downstream of Columbus. There is no evidence of anthropogenic gadolinium upstream of Columbus other than the relatively small gadolinium ratio increase at the Drake Union location. Further, both the field blank subtracted and non-subtracted gadolinium concentration measurements show a large increase when moving from within the city at Battelle River Front Park to the Jackson Pike Wastewater Treatment Facility downstream of Columbus. These results suggest that the city of Columbus does contribute anthropogenic gadolinium to the Scioto and Olentangy River system. Of the maximum total gadolinium concentrations measured (0.047 ppb – 0.064 ppb), the maximum estimated anthropogenic gadolinium concentration is about 0.040 ppb.

Suggestions for Future Work

First, a reanalysis and new preparation of the collected water samples and standards to avoid contamination would reduce concentration uncertainties. By eliminating any contamination throughout the samples, more accurate anthropogenic measurements can be identified and the full REE concentration pattern recorded. However, it is unlikely to change the main conclusions about the presence of anthropogenic gadolinium.

Following this reanalysis, future studies could obtain water samples from the many tributaries of the Scioto and Olentangy River systems that were not measured throughout our sampling group. These sources could give further information into the complete dissolved REE chemistry of the Scioto and Olentangy river systems, identifying any other possible source of anthropogenic gadolinium while also refining our conclusions. Further, specifically measuring just upstream of the Jackson Pike Waste Water Treatment Plant to declare the suspected entrance of the city's anthropogenic gadolinium would also improve our study. The potential for hospital treated waste water effluent to contribute anthropogenic gadolinium should be investigated.

All of our samples were acquired on a single day. By sampling at different periods throughout the year or over consecutive years into the future, this could give insight into seasonal and long term concentration changes. Environmental influences such the river's flow rates and how heavy precipitation seasons affect the measured concentrations could also be investigated.

Lastly, the influence of the bedrock geology on all of the REEs could also be explored. Further studies into the underlying rock units and their effects on the general REE chemistry are important. Further, pH effects influenced by the underlying rock units and by temperature may have significant affects upon the relative REE concentrations measured. From this, the pH should be measured in-situ during the sampling process to obtain the naturally accurate pH.

REFERENCES CITED

Bau, M., 1991, Rare-earth element mobility during hydrothermal and metamorphic fluid-rock interaction and the significance of the oxidation state of europium: Chemical Geology, v.93, p.219-230, doi: 10.1016/0009-2541(91)90115-8

Bau, M., Knappe, A,. Dulski, P., 2006, Anthropogenic gadolinium as a micropollutant in river waters in Pennsylvania and Lake Erie, northeastern United States: Chemie der Erde, v.66, p.143-152, doi:10.1016/j.chemer.2006.01.002

Bellin, M., Van Der Molen, A., 2008, Extracellular gadolinium-based contrast media: An overview: European Journal of Radiology, v.66, p. 160-167, doi:10.1016/j.ejrad.2008.01.023

Fitzgerald, W., Davidson, C., 1999, Clean Hands: Clair Patterson's Crusade Against Environmental Lead Contamination, Nova Science Publ. (1999), pp. 119-137

Gaines, P., Container Material Properties, Trace Analysis Guide: Part 5: https://www.inorganicventures.com/container-material-properties (Accessed May 2018).

Hatje, V., Bruland, K., Flegal, A., 2016, Increases in Anthropogenic Gadolinium Anomalies and Rare Earth Element Concentrations in San Francisco Bay over a 20 Year Record: Environmental Science and Technology, v.50, p. 4159-4168, doi: 10.1021/acs.est.5b04322

Humphris, S., 1984, The Mobility of Rare Earth Elements in the Crust: Developments in Geochemistry, *in* Henderson, P., Developments in Geochemistry v.2, p. 317-342, doi:10.1016/B978-0-444-42148-7.50014-9

Jarvis, K., Gray, A., McCurdy, E., 1989, Avoidance of Spectral Interference on Europium in Inductively Coupled Plasma Mass Spectrometry by Sensitive Measurement of the Doubly Charged Ion: Analytical Atomic Spectrometry, v.4 p. 743-747, doi:10.1039/JA9890400743

Klaver, G., Verheul, M., Bakker, I., Petelet-Giraud, E., Negrél, P.,, 2014, Anthropogenic Rare Earth Element in Rivers: Gadolinium and lanthanum. Partitioning between the dissolved and particulate phases in the Rhine River and spatial propagation through the Rhine-Meuse Delta (the Netherlands): Applied Geochemistry, v.47, p.186-197, doi:10.1016/j.apgeochem.2014.05.020

Kulaksiz S., Bau, M., 2011, Anthropogenic gadolinium as a microcontaminant in tap water used as drinking water in urban areas and megacities: Applied Geochemistry, v.26, pg. 1877-1885, doi:10.1016/j.apgeochem.2011.06.011

Longerich, H., Fryer, B., Strong, D., Kantipuly, J., 1987, Effects of operating conditions on the determination of the rare earth elements by inductively coupled plasma-mass spectrometry (ICP-MS): Spectrochimica Acta., v.42B, p. 75-92

Raab, M.S., 2005, The Investigation of High Performance Techniques and Application to Complex Matrices Using Inductively Coupled Plasma Mass Spectrometry and the Impact of Urbanization on the Scioto River System [PhD. Dissertation]: The Ohio State University, 456 p.

Taylor, S., McLennan, S., 1985, The Continental Crust: its Composition and Evolution: An Examination of the Geochemical Record Preserved in Sedimentary Rocks, Oxford, London. Blackwell Scientific Publications p. 29-42.

APPENDIX

Table A1. Concentrations of REEs in chondrite and shale standards (ppm). Chondrite – (Longerich & Fryer, 1987). PAAS, NASC, ES - (Taylor & McLennan, 1985).

	Chondrite	Post Archean average Australian Shale (PAAS)	North American Shale Composite (NASC)	European Shale (ES)
Nd	0.63	32.0	33.0	40.1
Sm	0.2	5.6	5.7	7.3
Eu	0.077	1.1	1.24	1.52
Gd	0.28	4.7	5.2	6.03
Tb	0.05	0.77	0.85	1.05
Dy	0.34	4.4	5.8	*
Ho	0.077	1.0	1.04	1.2
Er	0.23	2.9	3.4	3.55
Tm	0.035	0.4	0.5	0.56
Yb	0.22	2.8	3.1	3.29
Lu	0.034	0.43	0.48	0.58

Table A2. pH measurements of each sample.

Location number*	**Sample**	**pH**	**Location number***	**Sample**	**pH**
#1	LR-B	8.51	#9	S-B	8.21
#2	P-B	8.37	#10	CP-B	8.19
#3	DD-B	8.12	#11	C-B	8.38
#4	K-B	8.53	#6	FB-1 B	5.76
#5	D-B	8.32	#3	FB-2 B	5.76
#6	RF-B	8.24	#7	FB-3 B	5.76
#7	B-B	8.37	#9	FB-4 B	5.80
#8	JP-B	8.22	#11	FB-5 B	5.73

Table A3. Measured REE concentrations (ppb, ng/mL) without field blank subtraction.

	Ave Field Blank	**LR**	**P**	**DD**	**K**	**D**	**B**	**RF**	**JP**	**S**	**CP**	**C**
Loc. #		#1	#2	#3	#4	#5	#6	#7	#8	#9	#10	#11
^{141}Pr	*0.017*	0.014	0.015	0.019	0.013	0.018	0.014	0.019	0.021	0.019	0.018	0.017
^{143}Nd	*0.017*	0.022	**0.025**	**0.039**	0.019	**0.042**	0.017	**0.044**	**0.057**	**0.047**	**0.041**	**0.036**
^{145}Nd	*0.017*	0.018	**0.023**	**0.038**	0.017	**0.040**	0.017	**0.042**	**0.056**	**0.045**	**0.040**	**0.033**
^{147}Sm	*0.017*	0.015	0.017	0.021	0.014	0.022	0.015	0.022	0.025	0.023	0.021	0.020
^{149}Sm	*0.016*	0.015	0.016	0.020	0.015	0.021	0.014	0.021	0.025	0.022	0.021	0.019
^{151}Eu	*0.018*	0.021	0.021	0.021	0.024	0.022	0.021	0.020	0.021	0.020	0.021	0.023
^{153}Eu	*0.018*	0.026	0.026	0.025	0.033	0.027	0.027	0.025	0.025	0.024	0.027	0.030
^{156}Gd	*0.018*	0.017	**0.022**	**0.023**	0.017	**0.031**	**0.031**	**0.026**	**0.064**	**0.062**	**0.063**	**0.047**
^{157}Gd	*0.017*	0.016	**0.021**	**0.022**	0.017	**0.029**	**0.030**	**0.025**	**0.062**	**0.057**	**0.059**	**0.044**
^{158}Gd	*0.017*	0.016	**0.021**	**0.023**	0.016	**0.031**	**0.032**	**0.026**	**0.067**	**0.063**	**0.064**	**0.048**
^{160}Gd	*0.017*	0.018	**0.023**	**0.023**	0.018	**0.031**	**0.030**	**0.026**	**0.064**	**0.061**	**0.063**	**0.047**
^{159}Tb	*0.017*	0.013	0.015	0.015	0.013	0.016	0.014	0.015	0.016	0.015	0.015	0.015
^{163}Dy	*0.017*	0.016	**0.019**	**0.021**	0.016	**0.023**	0.015	**0.023**	**0.027**	**0.024**	**0.023**	**0.021**
^{164}Dy	*0.016*	0.016	**0.019**	**0.021**	0.015	**0.023**	0.015	**0.022**	**0.027**	**0.023**	**0.023**	**0.021**
^{165}Ho	*0.016*	0.014	0.015	0.016	0.013	0.016	0.014	0.015	0.017	0.015	0.015	0.015
^{167}Er	*0.016*	0.015	**0.019**	**0.020**	0.015	**0.021**	0.015	**0.020**	**0.023**	**0.021**	**0.020**	**0.019**
^{168}Er	*0.017*	0.017	**0.020**	**0.020**	0.015	**0.022**	0.015	**0.020**	**0.023**	**0.021**	**0.020**	**0.019**
^{169}Tm	*0.016*	0.014	0.015	0.015	0.013	0.015	0.014	0.014	0.015	0.014	0.014	0.014
^{173}Yb	*0.011*	0.018	**0.021**	**0.021**	0.015	**0.021**	0.016	**0.020**	**0.023**	**0.022**	**0.021**	**0.019**
^{174}Yb	*0.011*	0.017	**0.020**	**0.020**	0.015	**0.022**	0.016	**0.021**	**0.023**	**0.021**	**0.021**	**0.020**
^{175}Lu	*0.011*	0.014	0.016	0.017	0.014	0.016	0.015	0.015	0.016	0.015	0.015	0.016

Concentrations in **bold** are significantly higher than the average in the Field Blanks.

Table A4. Calibration and Field Blank ICP-SFMS signal intensities (counts/s).

	Calibration Blank	Field Blank 1	Field Blank 2	Field Blank 3	Field Blank 4	Field Blank 5	Ave. Field Blank	%RSD Field Blank
^{141}Pr	*27*	5201	5089	5227	5192	5042	5150	1.6%
^{143}Nd	*30*	660	649	654	627	653	649	2.0%
^{145}Nd	*11*	429	463	447	428	433	440	3.4%
^{147}Sm	*45*	760	809	791	837	778	795	3.7%
^{149}Sm	*8*	696	685	697	691	727	699	2.3%
^{151}Eu	*58*	2686	2493	2560	2622	*3188*	2710	10.2%
^{153}Eu	*64*	2863	2793	2798	2837	*4046*	3067	17.9%
^{156}Gd	*106*	1219	1185	1235	1215	1205	1212	1.5%
^{157}Gd	*76*	1017	978	991	998	1010	999	1.5%
^{158}Gd	*36*	1352	1308	1323	1327	1329	1328	1.2%
^{160}Gd	*42*	1242	1269	1275	1273	1250	1262	1.2%
^{159}Tb	*295*	5191	5184	5248	5190	5151	5193	0.7%
^{163}Dy	*47*	1293	1298	1279	1322	1304	1299	1.2%
^{164}Dy	*33*	1566	1531	1541	1545	1591	1555	1.5%
^{165}Ho	*34*	5186	5003	5229	5022	5139	5116	1.9%
^{167}Er	*31*	1204	1123	1165	1176	1154	1164	2.5%
^{168}Er	*38*	1456	1400	1403	1412	1435	1421	1.7%
^{169}Tm	*57*	5247	5110	5195	5242	5193	5197	1.1%
^{173}Yb	*10*	827	841	832	841	859	840	1.5%
^{174}Yb	*17*	1686	1637	1711	1689	1658	1676	1.7%
^{175}Lu	*509*	5643	5567	5586	5655	5456	5581	1.4%

Table A5. Ratio of Field Blank signal (count/s) to Calibration Blank signal (counts/s).

	Field Blank				
	1	2	3	4	5
^{141}Pr	193	188	194	192	187
^{143}Nd	22	22	22	21	22
^{145}Nd	39	42	41	39	39
^{147}Sm	17	18	18	19	17
^{149}Sm	87	86	87	86	91
^{151}Eu	46	43	44	45	55
^{153}Eu	45	44	44	44	63
^{156}Gd	12	11	12	11	11
^{157}Gd	13	13	13	13	13
^{158}Gd	38	36	37	37	37
^{160}Gd	30	30	30	30	30
^{159}Tb	18	18	18	18	17
^{163}Dy	28	28	27	28	28
^{164}Dy	47	46	47	47	48
^{165}Ho	153	147	154	148	151
^{167}Er	39	36	38	38	37
^{168}Er	38	37	37	37	38
^{169}Tm	92	90	91	92	91
^{173}Yb	83	84	83	84	86
^{174}Yb	99	96	101	99	98
^{175}Lu	11	11	11	11	11

Table A6. Concentrations of REEs (ppb) measured in Field Blanks.

	Field Blank 1	Field Blank 2	Field Blank 3	Field Blank 4	Field Blank 5	Ave. Field Blank	%RSD Field Blank
^{141}Pr	0.0168	0.0165	0.0169	0.0168	0.0163	*0.0167*	1.6%
^{143}Nd	0.0176	0.0173	0.0175	0.0167	0.0174	*0.0173*	2.0%
^{145}Nd	0.0167	0.0180	0.0174	0.0166	0.0168	*0.0171*	3.4%
^{147}Sm	0.0165	0.0175	0.0171	0.0181	0.0168	*0.0172*	3.7%
^{149}Sm	0.0163	0.0160	0.0163	0.0162	0.0170	*0.0163*	2.3%
^{151}Eu	0.0177	0.0165	0.0169	0.0173	0.0211	*0.0179*	10.2%
^{153}Eu	0.0171	0.0167	0.0168	0.0170	0.0242	*0.0184*	17.9%
^{156}Gd	0.0177	0.0172	0.0180	0.0177	0.0175	*0.0176*	1.5%
^{157}Gd	0.0177	0.0170	0.0173	0.0174	0.0176	*0.0174*	1.5%
^{158}Gd	0.0172	0.0166	0.0168	0.0169	0.0169	*0.0169*	1.2%
^{160}Gd	0.0164	0.0168	0.0168	0.0168	0.0165	*0.0167*	1.2%
^{159}Tb	0.0170	0.0170	0.0172	0.0170	0.0168	*0.0170*	0.7%
^{163}Dy	0.0166	0.0166	0.0164	0.0169	0.0167	*0.0167*	1.2%
^{164}Dy	0.0164	0.0161	0.0162	0.0162	0.0167	*0.0163*	1.5%
^{165}Ho	0.0165	0.0159	0.0166	0.0160	0.0163	*0.0163*	1.9%
^{167}Er	0.0169	0.0158	0.0164	0.0165	0.0162	*0.0164*	2.5%
^{168}Er	0.0170	0.0163	0.0164	0.0165	0.0167	*0.0166*	1.7%
^{169}Tm	0.0164	0.0160	0.0162	0.0164	0.0162	*0.0163*	1.1%
^{173}Yb	0.0159	0.0161	0.0160	0.0161	0.0165	*0.0161*	1.5%
^{174}Yb	0.0165	0.0160	0.0167	0.0165	0.0162	*0.0164*	1.7%
^{175}Lu	0.0179	0.0177	0.0177	0.0180	0.0173	*0.0177*	1.4%

Table A7. Reanalysis of field blank intensities (counts/s) before and after filtration.

Element	FB-1 Before filtration	FB-1 After Filtration
^{141}Pr	19	3583
^{143}Nd	67	495
^{145}Nd	7	286
^{147}Sm	81	613
^{149}Sm	5	501
^{151}Eu	78	1845
^{153}Eu	82	2046
^{156}Gd	69	869
^{157}Gd	85	712
^{158}Gd	35	902
^{160}Gd	106	938
^{159}Tb	171	3498
^{163}Dy	31	917
^{164}Dy	16	1069
^{165}Ho	14	3382
^{167}Er	17	830
^{168}Er	92	1028
^{169}Tm	90	3626
^{173}Yb	11	602
^{174}Yb	13	1157
^{175}Lu	289	3827

Table A8. Field blank subtracted REE concentrations (ppb, ng/mL) for samples from selected locations and REE elements.

	P	DD	D	RF	JP	S	CP	C
Loc. #	#2	#3	#5	#7	#8	#9	#10	#11
Nd	0.0065	0.0216	0.0241	0.0260	0.0394	0.0286	0.0231	0.0168
Gd	0.0046	0.0054	0.0134	0.0087	0.0472	0.0434	0.0451	0.0294
Dy	0.0025	0.0044	0.0062	0.0061	0.0101	0.0070	0.0062	0.0046
Er	0.0029	0.0035	0.0050	0.0037	0.0063	0.0043	0.0037	0.0024
Yb	0.0040	0.0047	0.0051	0.0042	0.0069	0.0049	0.0043	0.0031

Table A9. Background Equivalent Concentrations (ppt, pg/mL).

Pr141(LR)	0.087
Nd143(LR)	0.802
Nd145(LR)	0.428
Sm147(LR)	0.975
Sm149(LR)	0.187
Eu151(LR)	0.383
Eu153(LR)	0.383
Gd156(LR)	1.544
Gd157(LR)	1.327
Gd158(LR)	0.457
Gd160(LR)	0.555
Tb159(LR)	0.966
Dy163(LR)	0.603
Dy164(LR)	0.346
Ho165(LR)	0.108
Er167(LR)	0.436
Er168(LR)	0.443
Tm169(LR)	0.178
Yb173(LR)	0.192
Yb174(LR)	0.166
Lu175(LR)	1.619

Table A10. Calculated average gadolinium concentrations (ppb), estimated from all REE neighbors.

	JP	S	CP	C
Location #	#8	#9	#10	#11
Measured	0.038	0.038	0.040	0.029
Field Blank Subtracted	0.037	0.036	0.039	0.025